Active and Reactive Power Regulation in wind turbines based on BDFIG Machines.

Pablo E. Troncoso[1]
Instituto LEICI, Facultad de Ingeniería.
Universidad Nacional de La Plata, UNLP
Buenos Aires, Argentina.

Ricardo J. Mantz[2]
Instituto LEICI, Facultad de Ingeniería.
Universidad Nacional de La Plata, UNLP
Buenos Aires, Argentina.

Pedro E. Battaiotto
Instituto LEICI, Facultad de Ingeniería.
Universidad Nacional de La Plata, UNLP
Buenos Aires, Argentina.

***Abstract*. This papers deals with the control of active and reactive powers in wind energy conversion systems (WECS) powered by dual-stator-winding squirrel-cage induction generators (BDFIG). In these systems, the MPPT technics based on a torque control present coupling with reactive power objectives. A High Order Sliding Mode MIMO control is proposed for satisfying the power objectives in a decoupled way. The robustness of the Super Twisting MIMO controller is evaluated for different power requirements and wind profiles. A Pitch Angle Control allows extended the work range of WECS. The results are analyzed via simulations.**

Keywords—High Order Sliding Modes, Decoupling Control, BDFIG, WECS.

I. INTRODUCTION

The Doubly-Fed Induction Generator (DFIG) is one of the two most successful generators in wind energy industry. Among other reasons, its popularity is due to DFIGs only require partially rated power electronic converters to exchange active and reactive powers according to the real grid codes [1]. In despite of its popularity, researches continuously work for developing new doubly-fed generators with capability to recover slip power utilizing more reliable means than carbon brushes and slip rings and lesser requirements of gearbox.

In this way, the Brushless Doubly-Fed Induction Generator (BDFIG) arises as a viable alternative to DFIG machines in medium term [1][2]. This generator consists of two three-phase windings in the stator, usually called control and power magnetically coupled by a rotor squirrel cage nested. The absence of slip rings and brushes increases the system reliability and reduces the operational and maintenance costs. Additionally, due to their operational and constructive characteristics, the BDFIG can work with low mechanical speeds allowing a considerable reduction in the gearbox relationship or even its elimination. Likewise DFIG case, power converters controlling BDFIG only requires a fraction of the wind turbine rating [3].

Usually, generator torque and reactive power are basic requirements in wind energy conversion systems [3][4]. This paper addresses the control problem using High Order Slide Mode (HOSM) techniques, since they are particularly suited to cope with the coupling, model uncertainties and nonlinearities that arise along the extended operating region of the WECS evaluated in this paper. In fact, since its origin, Sliding Mode Control (SMC) has evolved into a robust and powerful design technique for a wide range of applications [5][6]. The most distinguished aspect of SMC is the discontinuous nature of its control action, providing excellent system performance, which includes insensitivity to certain parameter variations, rejection of matching disturbances [5]. Finite time convergent HOSMs preserve the features of the first order sliding modes and can improve them, if properly designed, by eliminating the chattering [7][8].

The structure of the paper is as follows. Section II introduces the mathematical model of the WECS powered by BDFIG. Section III discusses the HOSM MIMO control design, which is applied to the WECS in section IV. In section V the simulation results are presented and, finally, the conclusions are addressed.

II. WECS MODEL

The Fig.1 shows the topology of the WECS with BDFIG generator considered in this paper. While the stator power winding of the BDFIG machine is directly connected to the grid, the control stator winding is connected via a back-to-back converter [1].

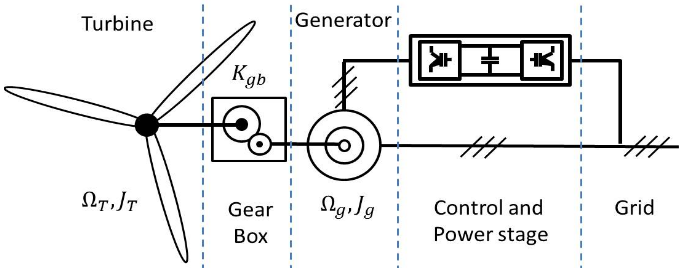

Fig.1 - WECS based on BDFIG in slip power recovery topology.

A. *dq-Model of the BDFIG Generator*

BDFIG can be modeled in a generic *dq* frame with six differential and six static equations that relate stator voltages, currents and magnetic fluxes [1].

Since the power winding is connected directly to the grid, the flux in it remains approximately constant. In this context, a good selection for the reference frame is $\lambda_p = \lambda_{dp}$ and $\lambda_{qp} = 0$, being λ_p the power winding flux. In the selected frame, the next equations relate the currents in the control and power windings

1 Consejo Nacional de Investigaciones Científicas y Técnicas (CONICET), (pablo.troncoso@ing.unlp.edu.ar).
2 Comisión de Investigaciones Científicas Provincia de Bs As(CICPBA).

$$\frac{di_{qc}}{dt} = -\frac{L_p r_r}{L_{mp}L_{mc}} i_{qp} - \frac{\sigma L_r L_p}{L_{mp}L_{mc}}\frac{di_{qp}}{dt} - \omega_1 i_{dc} - \frac{\sigma L_r L_p}{L_{mp}L_{mc}}\omega_1 i_{dp} + \frac{L_r}{L_{mp}L_{mc}}\omega_1 \lambda_p \qquad (1)$$

$$\frac{di_{dc}}{dt} = -\frac{L_p r_r}{L_{mp}L_{mc}} i_{dp} - \frac{\sigma L_r L_p}{L_{mp}L_{mc}}\frac{di_{dp}}{dt} - \omega_1 i_{qc} - \frac{\sigma L_r L_p}{L_{mp}L_{mc}}\omega_1 i_{qp} + \frac{L_r}{L_{mp}L_{mc}}\frac{d\lambda_p}{dt} \qquad (2)$$

where $$\omega_1 = \omega_e - p_p\omega_r \qquad \sigma = 1 - \frac{L_{mp}^2}{L_p L_r} \qquad (3)\ (4)$$

and the subscripts p, c and r stand for 'power winding', 'control winding' and 'rotor winding' quantities, respectively, and r_i, L_i and L_{mi} are the resistance, self-inductance and mutual inductance of the windings. The pole pair numbers are represented by p_i. Finally, ω_e and ω_r are the synchronous and rotational speeds, respectively.

Then, the expressions of active and reactive powers in the *dq* frame

$$P_p = \frac{3}{2}\left(v_{qp}i_{qp} + v_{dp}i_{dp}\right) \quad Q_p = \frac{3}{2}\left(v_{qp}i_{dp} - v_{dp}i_{qp}\right) \qquad (5)\ (6)$$

become in

$$P_p = \frac{3}{2}\frac{\omega_e}{\sigma L_r L_p}\left(-\frac{r_r}{\omega_1}\lambda_p^2 - L_{mp}L_{mc}\lambda_p i_{qc}\right) \qquad (7)$$

$$Q_p = \frac{3}{2}\frac{\omega_e\lambda_p}{\sigma}\left(\frac{1}{L_p}\lambda_p - \frac{L_{mp}L_{mc}}{L_r L_p} i_{dc}\right) \qquad (8)$$

being functions of the current components i_{qc} and i_{dc} of the control winding. Similarly, the instantaneous electromagnetic torque

$$T_g = \frac{3}{2}p_p L_{mp}(i_{qp}i_{dr} - i_{dq}i_{qr}) + \frac{3}{2}p_c L_{mc}(i_{qc}i_{dr} - i_{dc}i_{qr}), \qquad (9)$$

can be expressed in terms of these components as

$$T_g = \frac{3}{2}i_{qp}\left(p_c\frac{L_{mc}L_p}{L_{mp}}i_{dc} + p_p\lambda_p\right) + \frac{3}{2}\frac{p_c L_{mc}}{L_{mp}}i_{qc} \ . \qquad (10)$$

In Fig.2 is shown the steady-state torque characteristic for the BDFIG generator considered in this paper with the power winding connected to the 440 *Vrms* and 60 Hz grid and with the control winding shorted (i.e. $vc=0$). This torque results from the sum of the torques of the two stator windings (power and control windings). Besides displaying substantive differences with other induction machines, the torque curve stands out the strong non-linear characteristic of the BDFIG machine.

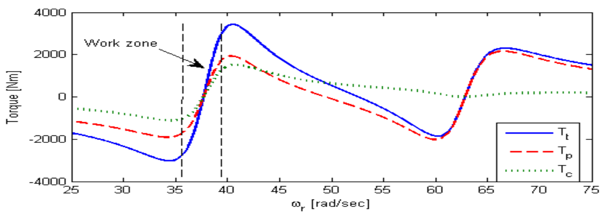

Fig.2 - Total torque (solid line), torque of the power winding (dashed line) and torque of the control winding (dotted line).

B. *Two mass model for WECS*

As widely used in the literature, a third order model capturing the first vibration mode of the drive train is taken into account. The model that considers two mass linked by a flexible shaft being its differential equations

$$J_T\dot{\Omega}_T = T_T - T_s \qquad J_g\dot{\Omega}_g = T_s - T_g \qquad \dot{\theta} = \Omega_T - \Omega_g \qquad (11)$$

where J_T and J_g are the turbine and generator inertias, Ω_T and Ω_g are the turbine and generator rotational speeds, T_T and T_g are the aerodynamic torque and electromagnetic torque of the generator, respectively, and T_s is the shaft torque

$$T_s = k_s\theta + k_b\dot{\theta} \qquad (12)$$

being k_s is the stiffness coefficient, k_b is the damping coefficient and θ is the angular deviation.

III. Control Strategy for the WECS Powered by BDFIG

The control strategy is based on in the idea of maximizing the extracted wind power maintaining the operation of the system within their rated limits, and simultaneously, to regulate the reactive power according to the grid demand.

Recently proposed, finite time convergent High Order Sliding Modes preserve the features of the first order sliding modes and improve them by eliminating the chattering [6][8]. In the past decade, the convergence and robustness of different HOSM controllers in multi-objective problems have been studied. In this context, these ideas are applied to design a decoupling HOSM control for the BDFIG generator.

Generator Control

As was commented in section II, the *dq* frame selected allows modeling the BDFIG machine with only four differential equations. Effectively, the reduced model can be written as

$$\frac{dx}{dt} = -L^{-1}Rx + L^{-1}Gu - L^{-1}G_p\tilde{v} = f(x,t) + \delta_f(x,t) + [g(x,t) + \delta_g(x,t)]u \qquad (13)$$

where

$$x = \begin{bmatrix} i_{qc} \\ i_{dc} \\ i_{qp} \\ i_{dp} \end{bmatrix} \qquad u = \begin{bmatrix} v_{qc} \\ v_{dc} \\ 0 \\ 0 \end{bmatrix} \qquad \tilde{v} = v_{dp},$$

The functions δ_f and δ_g represent additive disturbances and modeling errors. The term $L^{-1}Gu$ exposes as the control signals act on the dynamics of the stator winding currents, being its expression

$$L^{-1}G = \begin{bmatrix} \dfrac{L_{mp}^2 - L_p L_r}{\beta_1} & 0 \\ & \dfrac{L_r r_d - L_{mp} r_d + L_p L_r \omega_e}{\beta_2} \\ 0 & \\ \dfrac{L_{mc} L_{mp}}{\beta_1} & 0 \\ & \dfrac{L_{mc} L_{mp} \omega_e}{\beta_2} \\ 0 & \end{bmatrix} = \left[B\right]_{i,j} \quad (14)$$

where

$\beta_1 = L_p L_{mc}^2 + L_c L_{mp}^2 - L_c L_p L_r$,

$\beta_2 = r_d L_{mc}^2 + L_c L_{mp} r_p - L_c L_p r_d + L_{mc}^2 L_p \omega_e - L_c L_p L_r \omega_e$.

The chosen sliding surfaces are $S = \left[s_1 \quad s_2\right]^T$ with

$$s_1 = \begin{cases} T_g - T_{ref} & T_{ref}\omega_r \le P_{nom} \\ T_g - P_{nom}/\omega_r & T_{ref}\omega_r > P_{nom} \end{cases} \quad (15)$$

$$s_2 = Q_p - Q_{ref} \quad (16)$$

where Q_p and T_g correspond to (8) and (10), P_{nom} is the nominal power of the generator, Q_{ref} respond to the grid requirements and $T_{ref}=T_{opt}$ being

$$T_{opt}(\omega_r) = \frac{1}{2}\pi\rho r^5 \frac{C_p(\lambda_{opt},\beta)}{\lambda_{opt}^3}\omega_r^2 \quad (17)$$

for avoiding the wind speed measurement.

From trivial calculations, it is easy to see that the control objectives are relative degree 1 respect to v_{dc} and v_{qc}.

For tuning the second order sliding algorithm, time-derivate can be analyzed. The first time-derivate of sliding surfaces can be expressed as

$$\frac{dS}{dt} = \tilde{F}(x,t) + \tilde{G}(x,t)u + \tilde{\Delta}(x,t,u) \quad (18)$$

If the disturbance term (18) is bounded and the signal

$$u = \tilde{G}^{-1}(x,t)v \quad (19)$$

decouples (18) and the new control signal v can be tuned as m SISO controllers. For this problem, $\tilde{G}(x,t)$ depends only the electrical parameters in the next form

$$\tilde{G}(x,t) = \frac{dS}{dx}L^{-1}G = \begin{bmatrix} \frac{3}{2}(\gamma_1 i_{dc} + \gamma_2)B_{3,2} + \frac{3}{2}\gamma_3 B_{1,1} & \frac{3}{2}\gamma_1 i_{qp} \\ 0 & \frac{3}{2}\gamma_4 B_{2,2} \end{bmatrix} \quad (20)$$

where

$$\gamma_1 = \frac{p_c L_{mc} L_p}{L_{mp}}\ ;\ \gamma_2 = p_p \lambda_p\ ;\ \gamma_3 = \frac{p_c L_{mc}}{L_{mp}}\ ;\ \gamma_4 = -\frac{\lambda_p \omega_e p_c L_{mp} L_{mc}}{\sigma L_p L_r}\ .$$

In this context, a *Sliding Modes* algorithm provides rejects disturbances and modeling errors that the system under study may have, for example a variation in the frequency and voltage of the grid to which it is connected.

The control signals v_i are synthetized via a *Super Twisting* (*ST*) algorithm as

$$v_i = x_i - a_i\left|s_i\right|^{0.5}\operatorname{sgn}(s_i) \quad , \quad \dot{x}_i = -b_i \operatorname{sgn}(s_i)\ . \quad (21)$$

In this work, an adjustment of the gains of the *Super Twisting* algorithm through a *Lyapunov* approach is chosen, guaranteeing the stability and convergence of the control objectives. To be able to find such guarantees, the system has to comply with certain conditions that will be taken into account.

If the change of variables $T(S,\zeta,t) = x$ exists, and

$$\left\|\tilde{\Delta}(S,\zeta,t,u)\right\| \le \rho_i \left|s_i\right|^{0.5}.$$

When the parameters a_i and b_i are tuned as

$$a_i > 2\rho_i \quad b_i > a_i \frac{5\rho_i a_i + 4\rho_i^2}{2(a_i - 2\rho_i)}, \quad (22)$$

the control signal ensure the convergence to the sliding manifold $\dot{s}_i = s_i = 0$,

The *ST* algorithm is tuned in the next form

$$a_1 > 600 \quad a_2 > 1000 \quad b_1 > 3000000 \quad b_2 > 15000000;$$

for $\rho_1 = 200$ and $\rho_2 = 450$.

Via simulation, the bounds of disturbances in the dynamic expression of the sliding surfaces (15) and (16) give these ρ_i.

The *ST* algorithm provides robustness and a smooth control signal. This way of tuning the parameters of the controller is simpler than the traditional way since it requires less information about the successive derivatives of the sliding surface.

IV. RESULTS

The control of the system shown in Fig. 1 is evaluated by simulations. The power winding is connected to the *440 Vrms* and *60 Hz* grid and the control winding is connected to the grid via a PWM converter. The wind conversion system is designed to work with maximum mechanical power P_{mec}*=75 kw* from $\omega_r = 43.5\,rad/\sec$. The speed ω_r is modified with the reference power when this is lower than the rated power. The rated speed is $\omega_n = 47\,rad/\sec$. A realistic wind speed profile is considered, that forces the WECS to work in three regions of operation. Fig.3 shows the active and reactive power references change as follows:

- the reactive power reference changes at *40* and *250* seconds with amplitudes of *8 kVar* each
- the control objective of the active power for t<90sec and t>170sec, is to maximize the extraction of power available in

the wind. Between 90 and 170 sec, the power available is greater than the rated power of the system, and the power reference is set at rated power. Fig. 4 shows wind power (dashed) and the active power in the primary winding (solid). For t<90 seconds, the active power follows the path of the maximum available power. After that, the reference is set at the nominal power. Fig. 5 shows reactive power in the primary winding (solid) and the reactive power reference system (dashed). Fig. 6 shows the electromagnetic torque of the generator (solid) and the optimum torque available for the proposed wind profile (dashed). The control algorithm regulates the electromagnetic torque to the optimal torque until 90 seconds. The torque reference slides on the corresponding power hyperbola, when power achieves the nominal value. Then, the torque decreases until that the rotor speed achieves its nominal value. At this point, the pitch control limits the rotor speed as illustrated in Fig. 7. The upper and half box of Fig. 8 show v_{dc} and the v_{qc}. Notice how both signals help regulate the two control objectives. Finally, the bottom box shows how the pitch control limits the rate at nominal.

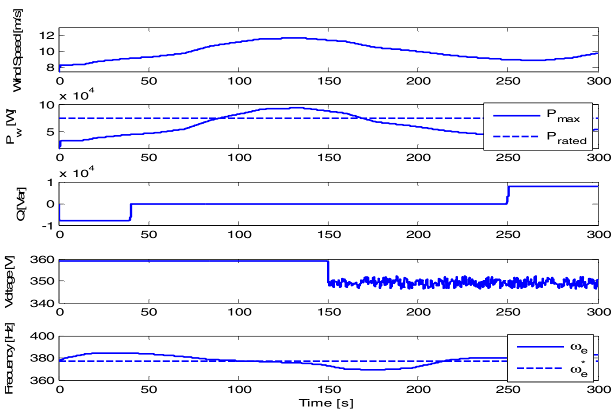

Fig.3 - Wind speed profile and power references scenario; Grid perturbations.

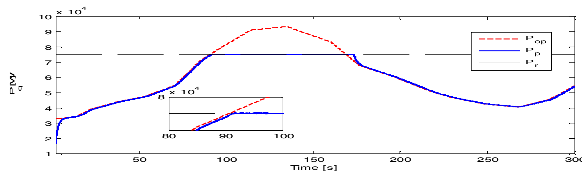

Fig.4 - Active power (solid), wind power (dotted) and rated power (dashed).

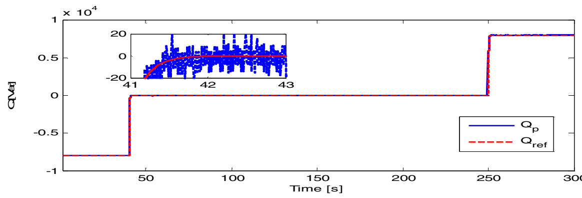

Fig.5 - Reactive power (solid), and reactive power reference (dashed).

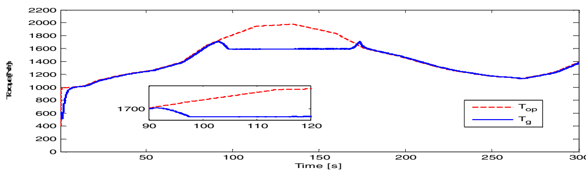

Fig.6 - Electromagnetic torque (solid line) and optimal torque (dashed line).

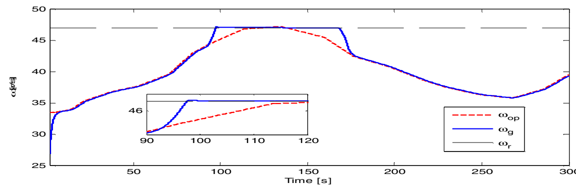

Fig.7 - Rotor speed (solid), optimal speed (dashed) and rated speed (dash-dot).

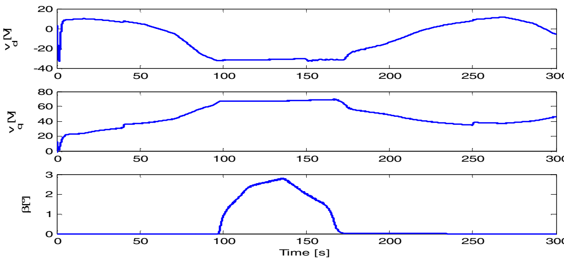

Figure 8. Time variation of the control signals.

V. Conclusion

BDFIG is a promising generator for powering low-maintenance WECS in many autonomous applications, and a viable alternative to the conventional generators in high power turbines. A strategy of HOSM with a multivariate approach is proposed in order to decouple electromagnetic torque and reactive power. In addition, the HOSM control copes with the characteristics presented by wind systems with BDFIGs, such as the nonlinear behaviors, and the presence of external perturbations and the random variability of the wind. From a practical point of view, the parameter tuning of the controllers is trivial without requiring information about the successive derivatives of the sliding surface as in the traditional case. Additionally, the flexibility of the super twisting algorithms allows extending work region to the full operation range of the WECS.

References

[1] H. Voltolini, "Modelagem e controle d geradores de inducao duplamente alimentados com aplicacao em eólicos", Florianópolis, Brasil`, 2007.

[2] F. Rüncos, R Carlson, A.M. Oliveira, P. Kuo-Peng and N. Sadowski, "Performance Analysis of a Brushless Double Fed Cage Induction Generator", *Nordic Wind Power Conf.*, Chalmers University, 2004.

[3] A. Singh and Mr. A. Gupta, "Performance Analysis of Wind Energy System Coupled with Brushless Doubly Fed Induction Generator and Matrix Convertor", *International Journal of Scientific and Engineering Research*, vol 5, issue 11, 2014.

[4] S. Hu and G. Zhu, "A vector control strategy of grid-connected brushless doubly fed induction generator based on the vector control of doubly fed induction generator", *IEEE Applied Power Electronics Conference and Exposition (APEC)*, 2016.

[5] F. Valenciaga and P. Puleston, "Variable Structure Control of a Wind Energy Conversion System Based on a Brushless Doubly Fed Reluctance Generator", *IEEE Tran. on Energy Conversion*, V.22, 2007.

[6] B. Beltran, M. El Hachemi Benbouzid and T. Ahmed-Ali "Second-Order Sliding Mode Control of a Doubly Fed Induction Generator Driven Wind Turbine", *IEEE Trans. on Energy Conversion*, Vol:27, Is: 2, 2012.

[7] J. Moreno and M. Osorio, "A Lyapunov approach to second-order sliding mode controllers and observers", *Proceedings of the 47th IEEE Conference on Decision and Control*, Cancún, México, 2008.

[8] L. Fridman, A. Levant . "Higher Order Sliding Modes". Chapter 3 in Sliding Mode Control in Engineering, pp. 53–101. Marcel Dekker, 2002.